17th World Conference on Earthquake Engineering, 17WCEE
Sendai, Japan - September 13th to 18th 2020

SEISMIC RATCHETING OF STEEL STRUCTURES WITH UNBALANCED STIFFNESS/STRENGTH

A. Rad[1], G. A. MacRae[2]

[1] *Structural Engineer, Aurecon New Zealand Limited, ali.rad@aurecongroup.com*
[2] *Professor, Tongji University, and Associate Professor, University of Canterbury, gregory.macrae@canterbury.ac.nz*

Abstract

Most structures built around the world have approximately the same stiffness/strength in both forward and backward horizontal loading directions. However, some structures may have different stiffnesses/strengths, and this means that the response from earthquake shaking in one direction will not be the mirror image of that from shaking in the other direction. Different stiffnesses/strengths in opposite horizontal directions can cause progressive yielding and displacements in one direction. This is sometimes termed ratchetting and the displacement demands may become significantly larger than for structures without a ratchetting tendency.

This study develops methods to estimate the peak and residual seismic displacements of steel structures with different stiffnesses in each direction. Inelastic dynamic time history analyses of 2-D steel frame building structures are conducted using a suite of ground motion records to evaluate their total response. An energy approach is used to estimate these displacements as a function of the relative stiffness/periods in the different directions and the lateral force reduction factor (R).

It is shown that with increased stiffness/strength in one direction (i) peak displacements in the stiffer direction tended to decrease and could be predicted by the spectral displacement associated with the period in that direction, (ii) the likely displacement in the flexible direction could be estimated from the displacement in the opposite direction using energy considerations, (iii) the median maximum peak displacement of the structure did not change, (iv) the residual drift decreased in the stiffer direction but, the absolute residual drift in the flexible direction was relatively unaffected by stiffness/strength increase. Design steps and an example are provided.

Keywords: seismic ratcheting, unbalanced stiffness/strength, peak and residual displacements, steel frame building

1. Introduction

Structures are usually designed to have the same stiffness/strength in forward and reverse horizontal directions because they are expected to perform similar ways under wind and earthquake loading. However, some structures may have different stiffness/strength in one horizontal direction compared to the opposite direction. Structures with significant unbalanced lateral force resistance have a tendency for inelastic deformation in predominantly one direction under strong earthquake shaking. This is sometimes termed ratcheting (e.g. MacRae 1994, Yeow et al. 2014, Rad et al. 2015, Rad et al. 2019). Some seismic standards (e.g. NZS1170.5:2016) have limitations on the permissible stiffness or strength difference to limit ratcheting. Nevertheless, many older structures, as well as newer structures in countries which do not have such provisions, may have stiffness/strength differences. For example, T-shaped reinforced concrete walls which are stiffer/stronger with the flange in tension than in compression, or structures with slender bracing elements not placed in a balanced configuration around the structure as shown in Fig. 1, may have a greater stiffness/strength in one direction than the opposite direction.

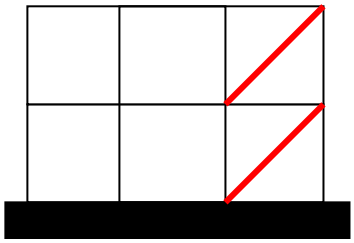

Fig. 1: Unbalanced Stiffness/Strength Building

Also, structures with residual displacements due to earthquakes may be strengthened/stiffened to limit the likelihood of further increase in displacement in that direction due to aftershocks. Such stiffening/strengthening can act as a permanent measure or as an interim measure, until the building is manually straightened and repaired, or deconstructed. While the concept regarding these mitigation measures is clear, simple methods to estimate the displacement demands of such structures with different strength/stiffness in the different directions are not available.

Based on the discussions above, it may be seen that there is a need to evaluate the likely seismic displacements of structures with different stiffness/strengths in opposite horizontal directions. In particular, answers are sought to the following questions:

1) How can the peak horizontal displacements in the stiffer direction be estimated?
2) How can the peak horizontal displacements in the flexible direction be estimated?
3) How do the peak absolute displacements change?
4) What procedures are appropriate for design?

2. Literature Review

The majority of previous studies used to estimate structural displacements response are for symmetric structures. They are based on an initial stiffness, or equivalent stiffness, which is the same in both directions. Such methods are difficult to generalize to structures with different stiffnesses in opposite directions. However, one approach which may be relevant considers energy concepts which are described below.

Housner (1956) stated that the earthquake energy transmitted into a structure, termed the input energy E_I, is defined as Eq. (1). This input energy consists of the kinetic energy (E_k), the potential energy (E_p) (consists of the recoverable elastic strain energy and the irrecoverable hysteretic energy) and damping energy (E_ξ). Kinetic

energy reflects the work of the inertia force; potential energy is the portion of the input energy stored in the structure, and damping energy is the work of the damping force.

$$E_I = E_k + E_p + E_\xi \quad (1)$$

Akiyama (1985) computed the input energy for a five-story building with different structural properties and also for an equivalent one-story building having the same fundamental period, total mass and yield strength using the S00E component of the 1940 El Centro record. He compared these two buildings and showed the total input energy transmitted to a five-story building is as much as the input energy transmitted to the equivalent one-story building, and consequently, it was concluded that input energy transmitted to one of them can be computed from the other. Akiyama (1985) also defined an energy spectrum based on the relationship between input energy and natural period of the system. He expressed input energy in terms of equivalent pseudo-velocity, V_E, which is defined in Eq. (2) where E_I is the input energy and M is the mass of the structure.

$$V_E = \sqrt{2E_I/M} \quad (2)$$

Akiyama (1985, 1988) suggested that a bilinear curve may be appropriate to provide the energy spectrum in terms of pseudo-velocity, V_E. For structures with low periods, T, V_E linearly increases with T and at higher T it becomes constant as shown in Fig 2. He also stated that the input energy spectrum obtained for elastically responding structures is also valid for inelastic systems with the total input energy in both cases being similar.

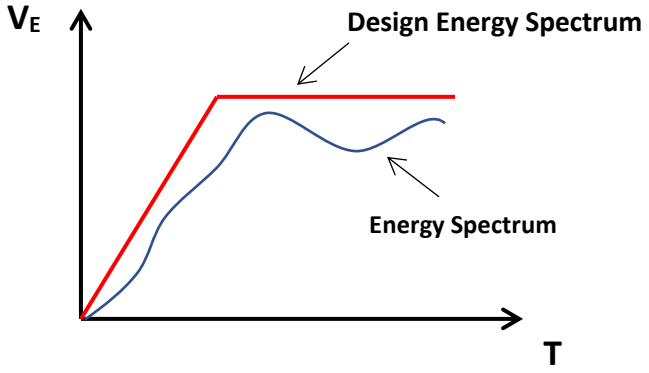

Fig 2: Energy Spectrum

Uang and Bertero (1990) showed that earthquake input energy may be obtained two ways; one based on the relative motion and the other on absolute motion. Uang and Bertero (1990) noticed a difference in the magnitude of relative and absolute input energies, E_k and E'_k, for the very short and long period structures. For long period structures the mass of the structure almost does not move. Therefore, the absolute input energy, E'_I, for the relatively long period structure should be low.

Chopra (1995) and Bruneau and Wang (1996) state that the relative motion input energy, E_I, is more meaningful than the absolute motion input energy, E'_I, since internal forces and damage within a structure are related to relative displacements and velocities. Bruneau and Wang (1996) also indicated that damping ratios smaller than 5% have a minor influence on input energy, E'_I.

Nakashima et al. (1996) investigated the effect of damping ratios and large post elastic stiffness ratios (up to 0.75) for bilinear SDOF and MDOF structures. They concluded that in general, damping and large post elastic stiffness ratios have a minor effect on the input energy.

While some studies have been conducted to determine the response of the structures with different strength in different directions (e.g. Yeow et al. 2013, Saif et al. 2017), or different stiffness in different directions for

elastic structures (Rad and MacRae, 20019), no studies are known to have specifically addressed the estimation of displacements of yielding structures with different stiffnesses/strength in opposite horizontal directions.

Priestley, et al. (2007) also argued that in many cases strength may be proportional to stiffness. This may be stated that the yield displacement, $\Delta_y = F_y/k$, is constant.

Moreover, Paulay and Priestly (1992) also showed that for structures with periods more than 0.7s, the ductility (μ) is often similar to force reduction factor (R). However, for structures with period less than 0.7s, they are not equal and a relationship between them was given in Eq. (3) which has been adapted in NZS1170.5. Here for a specific R value, by decreasing T, the corresponding μ is increased. Therefore, the ratio of (μ/R), is increased by decreasing the period T, of the structure. Eqs. (3) to (7) and Fig. 3 show that this ratio (μ/R) equals to ratio of ultimate to elastic displacement response (Δ_u/Δ_e). In Fig. 3, F_e and F_y are the elastic force response, and the yielding strength of the structure respectively. Also, Δ_e, Δ_y, and Δ_u are the elastic, yield and ultimate displacement of the structure. Thus, ratio of ultimate to elastic displacement response (Δ_u/Δ_e) is increased by decreasing the period, T, of the structure.

$$\mu = min\begin{cases} 1 + (R-1)\frac{0.7s}{T} \\ 1 \end{cases} \tag{3}$$

$$R = \frac{F_e}{F_y} = \frac{\Delta_e}{\Delta_y} \tag{4}$$

$$\mu = \frac{\Delta_u}{\Delta_y} \tag{5}$$

$$\Delta_y = \frac{\Delta_e}{R} \tag{6}$$

$$\frac{\Delta_u}{\Delta_e} = \frac{\mu}{R} = max\begin{cases} \frac{\left(1+(R-1)\frac{0.7s}{T}\right)}{R} \\ 1 \end{cases} \tag{7}$$

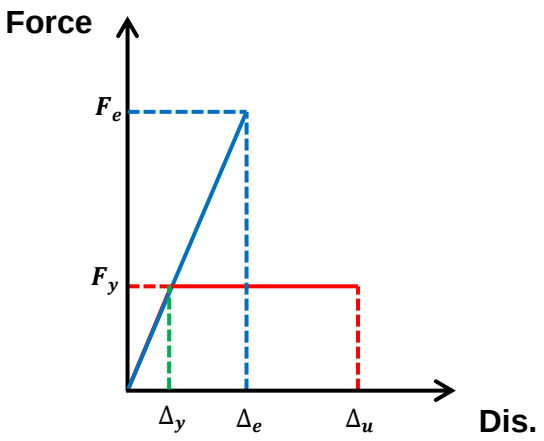

Fig. 3: Effect of R and μ on peak displacement response

3. Modelling and Evaluation Approach

In this study, both elastic and a nonlinear single-story steel frame structures are considered for analysis as shown in Fig. 4.The structure has a floor mass of 20 tonnes, floor height of 3m and a span length of 6m. For this model, the bases of the columns were modelled as pinned, and column stiffnesses was assumed to be constant with moments of inertia of 0.000388m^4 and modulus of elasticity of 200GPa each for all periods. Elastic structures with periods ranging from 0.5 to 5s are considered. For nonlinear structures, the basic structure was designed with target maximum interstory drifts of 1.5%, 2.0% and 2.5% and force reduction factors of 1, 2, 4 and 6 according to the equivalent static method in NZS1170.5 (2016). Changing of the design drift of the nonlinear structure is controlled by the beam stiffness. The periods of the nonlinear structure with these design drifts of 1.5%, 2.0% and 2.5% are 0.45s, 0.55s and 0.7s respectively.

To obtain unbalanced stiffness elastic structures, an "elastic tension-only" brace was added to the symmetric structure to increase stiffness in the stiffer direction, K_s, up to 10 times that in the more flexible direction, K_f. To make unbalanced nonlinear structures, a "nonlinear tension-only" brace with slackness was added to the structure to increase the stiffness ratio, $K_{ratio} = K_s/K_f$, from 1 to 10. The strength ratio was made the same as the stiffness ratio, K_{ratio}, following to Priestley et al. (2007) so balanced and unbalanced structures all have same yield displacement (Δ_y) as shown in the push-pull curve of the structures in Fig. 5. While providing a very high K_{ratio} may not be permitted for the design of a new building, it may be useful to limit the possibility of further positive displacements in a frame with an initial permanent positive displacement from a previous earthquake event. However, as this study relates to fundamental behaviour associated with different stiffness/strengths in opposite directions, no initial permanent displacement is explicitly considered here. The hysteretic behaviour was assumed to be elastic perfectly plastic.

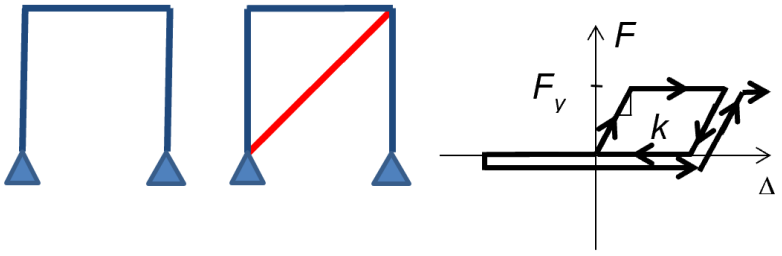

(a) Frame Building (b) Building with tension-only braces (c) Brace hysteresis loop

Fig. 4: Structure Models

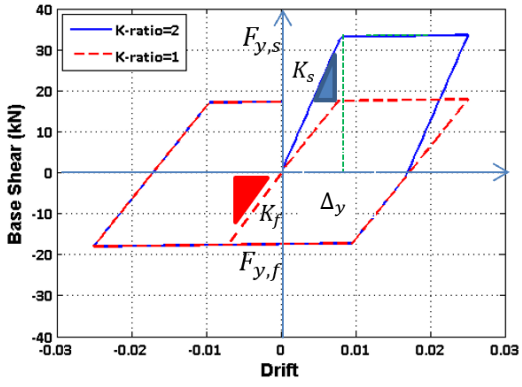

Fig. 5: Push-pull behavior of balanced (K_{ratio} = 1) and unbalanced (K_{ratio} = 2) stiffness/strength structures

The SAC (SEAOC-ATC- CUREE, 2000) suite of 20 earthquake ground motion records for Los Angeles, with a probability of exceedance of 10% in 50 years, was used. To eliminate directionality effects from individual ground motion records, analyses were repeated by applying the same ground motions in the opposite direction. All earthquake ground motions records are scaled to elastic design spectral acceleration at fundamental period of the frame structure without a brace.

The dynamic inelastic time history analysis was performed using OpenSees (2017). MATLAB (2008) was used to extract the peak displacement in both stiffer and more flexible directions. These are termed peak stiff displacement, *PSD*, and peak flexible displacement, *PFD*, respectively. Initial mass proportional Rayleigh damping, with a damping ratio of 5%, was considered. Damping ratios were specified as being proportional to the more flexible stiffness. Hysteresis loops were considered to already consider P-delta effects which were not explicitly considered.

The potential energies in the more flexible direction, PE_f, and stiffer direction, PE_s, were calculated using Eqs. (8) and (9) where K_f is the stiffness of the more flexible side, K_s is the stiffness of the stiffer side.

$$PE_f = K_f PFD^2/2 \quad (8)$$

$$PE_s = K_s PSD^2/2 \quad (9)$$

4. Seismic Energy Response of Elastic Structures

Fig. 6 shows the median spectral potential energy of the structures in the flexible direction, PE_f, and stiffer direction, PE_s, under 40 records with different K_{ratio} are approximately equal.

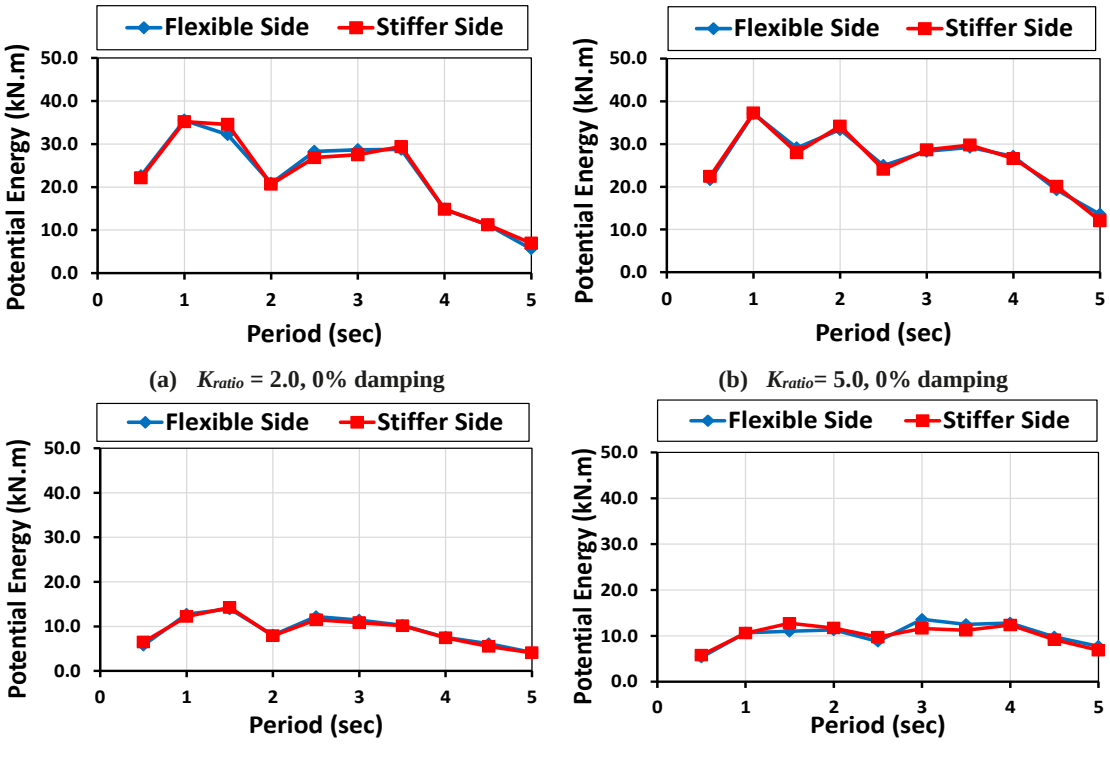

(a) K_{ratio} = 2.0, 0% damping

(b) K_{ratio}= 5.0, 0% damping

(c) K_{ratio} = 2.0, 5% damping

(d) K_{ratio} = 5.0, 5% damping

Fig. 6: Median spectral potential energy of the structures with different initial periods and K_{ratio} in stiff and flexible directions from 40 analyses using 20 SAC La10in50 records in both directions

Fig. 7 also shows the hysteresis loop of the structure with unbalanced stiffness ratio of 5 under the Imperial Valley (El Centro, 1940) ground motion record. It shows that displacement of the structure in the stiffer direction is less than in the more flexible one. Also, the base shear in stiffer direction is larger than in the other. Therefore, the potential energies in the stiffer and more flexible directions, which equal the area under the hysteresis loop ($PE_f \approx$ 0.285m*220kN/2=31, $PE_s \approx$ 0.14m*460kN/2=32kNm) are approximately equal.

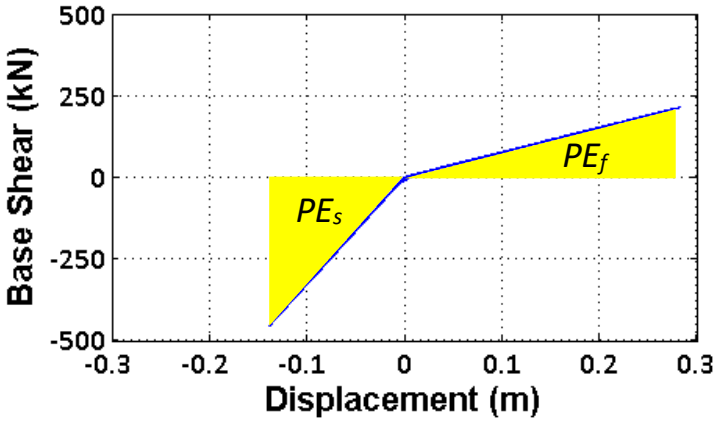

Fig. 7: Hysteresis loop of the structure with unbalanced stiffness (K_{ratio} =5.0) and initial period of 1s under la01 from SAC record (Imperial Valley, El-Centro, 1940), Damping=0%.

5. Seismic Displacement Response of Elastic Structures

Fig. 8 illustrates the trends shown above by plotting the *PSD* versus stiffer direction period, T_s, versus the period in the more flexible direction, T_f. For a linear structure, with $K_{ratio} = K_s/K_f = 1$, the stiffer direction period, T_s, is equal to T_f and this is indicated by the far right point on each line in Fig. 8. In this case, the response there is equal to the spectral displacement for this period, $T_f = T_s$ as expected. As the stiffness ratio, $K_{ratio} = K_s/K_f = (T_f/T_s)^2$, increases, K_s increases, and T_s decreases as shown in the figure. For increasing K_{ratio} (i.e. decreasing T_s), the peak stiff displacement, *PSD*, decreases indicating that increasing the stiffness in one direction decreases the displacements in that direction. This indicates the effectiveness of providing additional structural strength in one direction to limit displacements in that direction. Fig. 8 also shows that the designed spectral displacement, S_d, can be used to estimate the peak displacements in the stiffer direction although it is conservative at T_s values near 3s especially for very long period structures with $T_s \geq$ 4s.

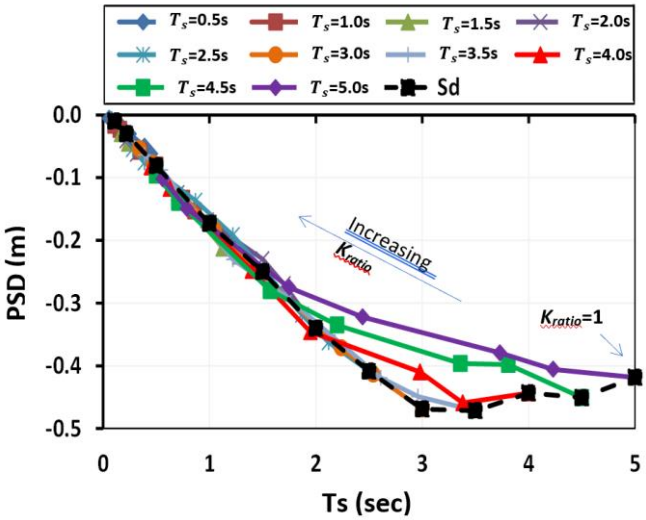

Fig. 8: Effect of K_{ratio} and T_s on PSD

Fig. 9 shows that the median *FSR*, defined as the ratio of flexible-to-stiffer displacement, computed as the peak flexible displacement, *PFD*, divided by the peak stiffer displacement, *PFD*, is independent of the period of the structures, T_f, and only changes with K_{ratio}. This can be explained based on the potential energy of the two sides of the structures explained in Section 4. As shown in Fig. 6 and Fig. 7 the potential energy in the positive (flexible) direction, PE_f, and negative (stiffer) directions, PE_s, are approximately equal. Therefore, based on Eqs. 8 and 9:

$$PFD = PSD \,.\, \sqrt{(K_s/K_f)} = PSD \,.\, T_f/T_s \quad (10)$$

For example, based on Fig. 9, the average computed *FSR* (= *PFD*/*PFD*) for K_{ratio} (=K_s/K_f) of 2, 5, 10, 100 is about 1.39, 2.2, 3.05 and 9.8 which is similar to the results of the Eq.10 which give 1.41, 2.23, 3.16 and 10 as shown on the beside the left hand axis of the figure.

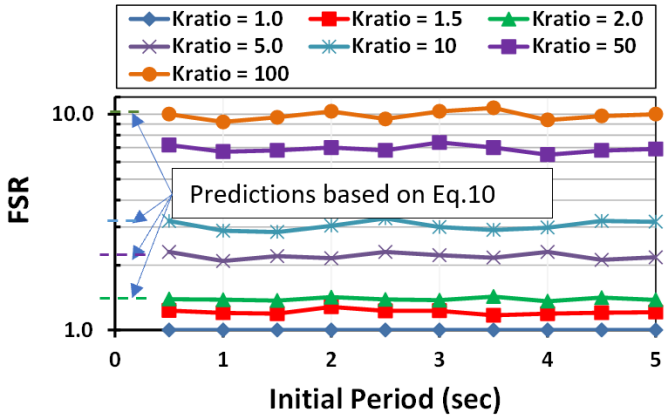

Fig. 9: Effect of K_{ratio} and initial period of the unbalanced structures on median FSR with 5% damping from 40 analyses using 20 SAC La10in50 records in both directions.

6. Seismic Displacement Response of Nonlinear Structures

6.1 Absolute Peak Drift Response

Fig. 10 shows that median absolute peak drift response of the structure considering both stiffer and more flexible directions (i.e. max{PSD, PFD}) changed less than 10% for K_{ratio} from 1.0 to 10. Generally the maximum drift in either direction was the PFD drift as shown above (i.e. max{PSD, PFD} = PFD). While increasing K_{ratio} the median PSD decreased, but the median PFD for different *R* values and design drifts does not change significantly.

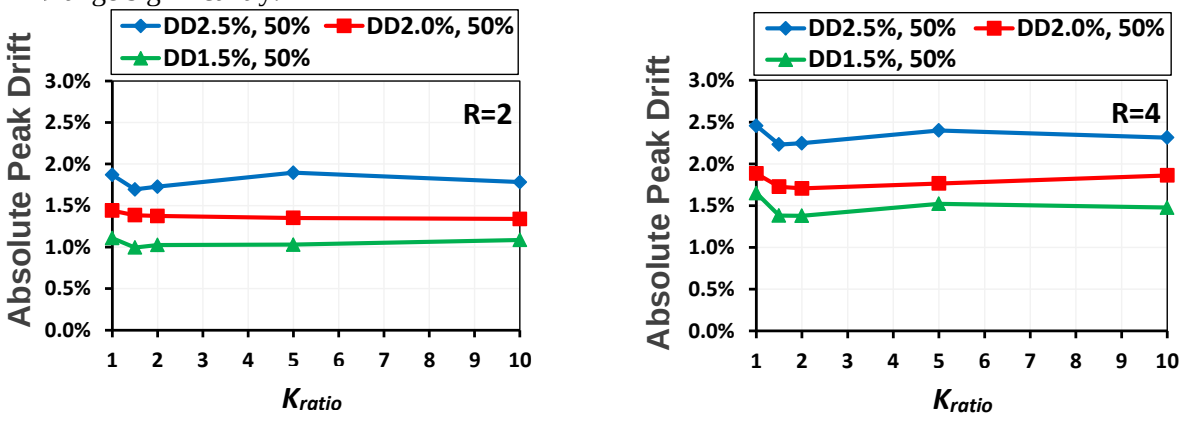

Fig. 10: Median absolute Peak Drift Response from 40 analyses using 20 SAC La10in50 records (both dir.).

6.2 Peak Stiffer Direction Drift Response

Fig. 11 shows that as K_{ratio} increases, the PSD tends to decrease. For K_{ratio} of 1, although the design drifts of the structures are 2.5%, 2.0% and 1.5%, the median PSD drifts are less than about 1.6%. This is because the maximum drift of the structure can occur in either direction under different earthquake records and shaking directions. Therefore, by choosing only one direction, the median peak drift of that direction is less than median maximum drift shown in

10.

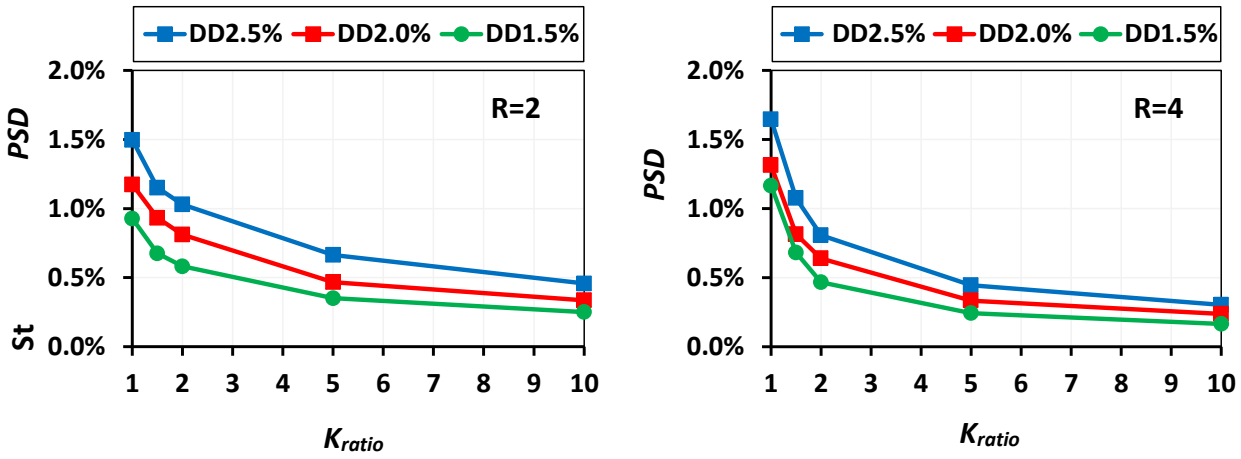

Fig. 11: Effect of K_{ratio}, Design drift and R on Peak Positive Drift (Stiffer direction) from 40 analyses using 20 SAC La10in50 records in both directions

6.3 Peak Flexible Direction Drift Response

Fig. 12 shows that the absolute peak drift in the flexible direction, PFD, can increase and become almost constant with greater K_{ratio}. This increase is greater with higher design drift and force reduction factors (R). For low design drifts and force reduction factors, R, PFD remains almost constant. This is consistent with an elastically responding structure.

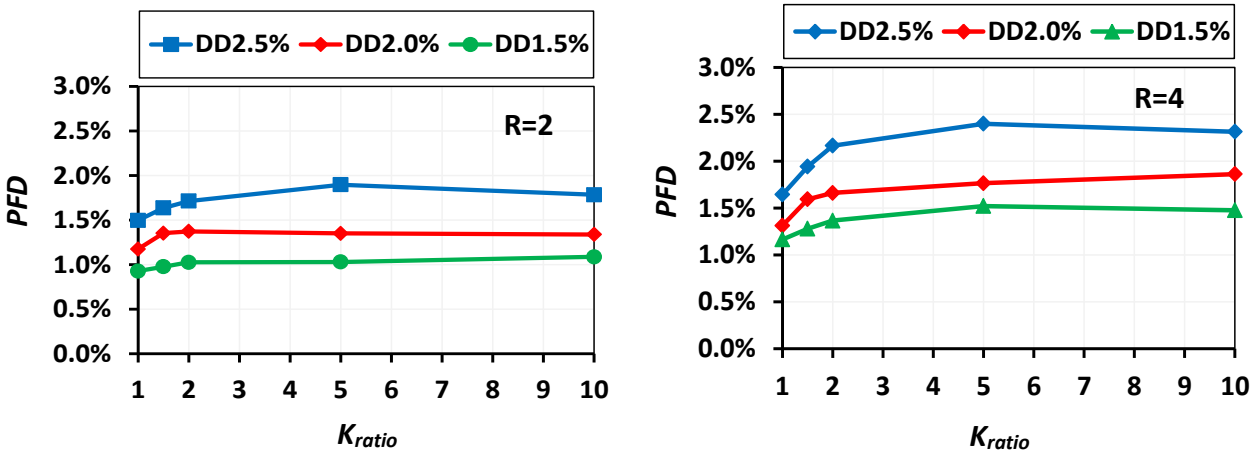

Fig. 12: Effect of K_{ratio}, Design drift and R on Median Peak Flexible Drift, PFD, from 40 analyses using 20 SAC La10in50 records in both directions

7. Design Considerations

A number of different methods could be proposed for design based on the relationships observed. One simple approximate proposal given below uses the observations that:

i) elastic peak displacements in the stiffer direction, elastic *PSD*, can be obtained by from the spectral displacements according to Fig. 8, and

ii) elastic peak displacements in the flexible direction, elastic *PFD*, can be obtained by from energy considerations according to Fig. 9, and

iii) the inelastic peak flexible displacement, *PFD*, does not change much with K_{ratio} according to Fig. 12.

Methodology is as follows:

Step 1: Estimate elastic displacement of the stiffer side, elastic *PSD* from *Sd* (*Ts*).
Step 2: Estimate elastic displacement of the flexible side from Eq.10, $PFD_e = PSD_e.\sqrt{(K_s/K_f)}$.
Step 3: For each direction, calculate inelastic displacements using Eq. 7. Here, *R* can be taken as $R_s = \frac{\Delta_{e,s}}{\Delta_y}$ for stiffer direction and $R_f = \frac{\Delta_{e,f}}{\Delta_y}$ for flexible direction from Eq.4 and Fig. 3 until further information is available. Here, based on Priestley, et al. (2007), Δ_y (yield displacement) is constant for both stiffer and flexible directions.

$$PSD = PSD_e \times max\begin{Bmatrix}\left(1+(R_s-1)\frac{0.7s}{T_s}\right)\\ R_s\\ 1\end{Bmatrix}$$

$$PFD = PFD_e \times max\begin{Bmatrix}\left(1+(R_f-1)\frac{0.7s}{T_f}\right)\\ R_f\\ 1\end{Bmatrix}$$

Example:

For a structure with mass of 20 tonnes, an initial design drift of 2.0%, periods, T_f, of 0.57s and T_s of 0.285s, story height of 3m, *R* of 4 and stiffness ratio, K_{ratio}, of 4.0, the likely PSD and PFD are calculated as:

Step 1: By assuming the design spectra is given by NZS117.5 for Wellington, soil type C, the elastic peak stiffer displacement, $\Delta_{e,s}$, of the unbalanced stiffness structure with T_s of 0.285s is PSD_e = 0.019m.

Step 2: The elastic peak more flexible displacement, PFD_e, equals to $0.019\times\sqrt{4}$ = 0.038m.

Step 3:

$$\Delta_y = {}^{V}/_{K} = {}^{c.w}/_{\left(\frac{4\pi^2 m}{T^2}\right)} = \frac{0.18\times9.81\times20{,}000}{2427725.45} = 0.0145$$

$$R_s = \frac{\Delta_{e,s}}{\Delta_y} = {}^{0.019}/_{0.0145} = 1.3$$

$$R_f = \frac{\Delta_{e,f}}{\Delta_y} = {}^{0.038}/_{0.0145} = 2.6$$

$$\Delta_{u,s} = 0.019\times(1+(1.3-1)\times\frac{0.7}{0.285})/1.3 = 0.019\times1.56 = 0.025\text{m}$$

$$\Delta_{u,f} = 0.038\times(1+(2.6-1)\times\frac{0.7}{0.57})/2.6 = 0.038\times1.76 = 0.043\text{m}$$

8. Conclusion

In this study, peak seismic displacements of nonlinear single-story structures with different stiffness/strength in opposite directions are obtained using response history analysis. Parameters considered were the relative stiffness/period in the different directions, the force design reduction factor (R), and the design drift. It was found that by increasing the stiffness/strength in one direction

(i) peak displacement in the stiffer direction tended to decrease and could be predicted by the spectral displacement associated with the period in that direction,

(ii) the likely displacement in a flexible direction could be estimated from the displacement in the opposite direction using energy considerations,

(iii) the median maximum peak displacement of the structure did not change,

(iv) a methodology to estimate peak displacements is developed that is consistent with current standards and with fully elastic response. An example is also provided.

9. References

[1] MacRae GA. P-Δ effects on single-degree-of-freedom structures in earthquakes. Journal of Earthquake Spectra, 1994; 10(3):539–568.

[2] Yeow TZ, MacRae GA, Sadashiva VK, Kawashima K. Dynamic stability and design of C-bent columns. Journal of Earthquake Engineering 2013; 17:5,750–768.

[3] Rad, A. A., MacRae, G., Bull, D. and Yeow, T. (2015). Seismic Behavior of Steel Buildings with Initial Out-of-Plumb. Earthquake Eng. Struct. Dyn., 44 (14), 2575-2588,

[4] Rad A. A., Hazaveh N. Kh., MacRae G. A., Rodgers G. W., Ma Q. (2019). Structural straightening with tension braces using aftershocks – Shaking table study, Soil Dynamics and Earthquake Engineering, 123, 399-412.

[5] NZS 1170.5:2016. Structural Design Actions Part 5: Earthquake Actions New Zealand. Standards New Zealand: Wellington, New Zealand, 2004.

[6] Housner G.W. Limit design of structures to resist earthquakes. Proc. of the 1st World Conference on Earthquake Engineering, California, USA, 1956, 5, pp. 5-1 to 5-13

[7] Akiyama H. Earthquake-resistant limit-state design for buildings. the University of Tokyo Press, Tokyo, Japan, 1985.

[8] Akiyama H. Earthquake-resistant design based on the energy concept. Proc. of the 9th World Conference on Earthquake Engineering, Tokyo-Kyoto, Japan, 1988.

[9] Uang C.-M., Bertero V. V. Evaluation of seismic energy in structures. Earthquake Eng. & Struct. Dyn, 1990, 19(1), pp. 77-90

[10] Chopra A. Dynamics of structures: Theory and applications to earthquake engineering. Perntice Hall, 1995.

[11] Bruneau M. and Wang N. Some aspects of energy methods for the inelastic seismic response of ductile SDOF structures. Eng. Struc., 1996, 18(1), pp. 1-12.

[12] Nakashima M., Saburi K., and Tsuji B. Energy input and dissipation behaviour of structures with hysteretic dampers. Earthquake Eng. & Struct. Dyn., 1996, 19(1), pp. 77-90.

[13] Saif, K.Z., Lee, C.L., MacRae, G.A., Yeow T.Z. (2017), Effect of eccentric moments on seismic ratcheting of single-degree-of-freedom structures, NZSEE conference, Christchurch, New Zealand.

[14] Priestley M.J.N., Calvi G.M., Kowalsky M.J. (2007), Direct displacement-based seismic design of structures NZSEE conference.

[15] Paulay and Priestly (1992), "Seismic design of reinforced concrete and masonry buildings", Willey, ISBN: 978-0-471-54915-4, 768 pages.

[16] SAC (SEAOC-ATC-CUREE) (2000), The SAC Steel Project. Berkeley, Ca.

[17] Rad, A.A. and MacRae, G. (2019) "Displacement estimation of elastic structures with unbalanced stiffness using energy approach". Journal of Earthquake Engineering 2019; 1-19.

[18] OpenSees (2017), Open System for Earthquake Engineering Simulation- Home Page: http://opensees.berkeley.edu/.

[19] The MathWork, Inc., Matlab R2008a.

